Appl. Phys. B 70, 833–837 (2000) / Digital Object Identifier (DOI) 10.1007/s003400000211

Applied Physics B
Lasers
and Optics

Measurement of the pulse-front distortion in high-numerical-aperture optics

R. Netz, T. Feurer*, R. Wolleschensky, R. Sauerbrey

Institut für Optik und Quantenelektronik, Friedrich-Schiller-Universität Jena, Max-Wien-Platz 1, 07743 Jena, Germany

Received: 11 October 1999/Revised version: 4 November 1999/Published online: 23 February 2000 –

Abstract. Using ultrashort laser pulses in combination with laser scanning microscopes offers the fascinating possibility to investigate samples with high spatial and temporal resolution. On the other hand the use of ultrashort pulses leads to pulse broadening and pulse-front distortion due to the dispersion of the optical elements. Three different experimental techniques are presented which are able to determine the pulse-front distortion for high-numerical-aperture objectives due to chromatic and spherical aberration. Results for a number of widely used objectives are listed.

PACS: 32.23.-b

Although optical microscopy has been used for centuries, in the last decades several novel techniques, such as confocal microscopy or two-photon microscopy, have been developed. Two-photon microscopy is a relatively new method that has become possible with the development of short-pulse lasers [1, 2]. Recent experimental results have, however, shown that in principle it also works with continuous wave lasers [3] of course at the expense of temporal resolution. In two-photon microscopy dyes or fluorochromes are excited by the simultaneous absorption of two photons and the fluorescence light is subsequently detected. One major advantage of two-photon excitation over one-photon excitation is that the depth resolution is provided by the excitation process rather than by the detection system. The intensity is high enough to excite the molecules in the small focal volume only. This leads to the possibility to record three-dimensional images in relatively thick samples ($> 100\,\mu$m). If ultrashort pulse lasers are used the high spatial resolution is accompanied by a high temporal resolution, which in turn offers fascinating new possibilities. Since ultrashort pulses have a comparatively large spectral bandwidth dispersion effects in the optical elements of the microscope lead to considerable pulse broadening [4, 5] and presumably also to pulse-front distortion [6]. Therefore, it is necessary to measure and compensate for these effects in order to ensure optimum performance. Using a suitable prechirp unit it has been possible to compensate for the pulse broadening [4] even for sub-10-fs pulses [5, 7]. On the other hand chromatic and spherical aberrations lead to a radius-dependent group delay [6] and, therefore, different radial portions of the beam arrive at different times at the focal region and cause a temporal broadening of the pulse in the focal region.

In the following, experimental results are presented which investigate the effects of chromatic and spherical aberration in a microscope on the group delay of a femtosecond pulse. In contrast to previous measurements, three different experimental techniques have been used to measure the group delay as a function of the beam radius assuming cylindrical symmetry, i.e. spatial and spectral interferometric techniques and an autocorrelation technique, respectively. The different methods are compared to approximate analytic calculations and to ray tracing calculations.

1 Experimental methods

First, the experimental setup is presented, and second, the three different methods which have been used to measure the pulse-front distortion are described in detail. The experiments were performed using the arrangement shown in Fig. 1, employing a home-built fs laser oscillator. The Ti:sapphire laser system (800 nm, 105 MHz, 400 mW, 36 nm spectral bandwidth) was pumped by a frequency-doubled cw 5-W Nd:YAG laser. The output laser beam was directed into a Michelson interferometer. Before entering the interferometer, the pulses were sent in an external prism compressor consisting of SF10 prisms. The minimum time–bandwidth product that has been achieved after the SF10 prism compressor was 0.49 assuming a sech^2 pulse shape. This corresponds to a pulse width of 32 fs. For most experiments the beam size was expanded by an all reflective $6\times$ telescope in order to obtain a beam diameter of about 10 mm. The microscope objectives were placed in the object arm of the Michelson interferometer and in the reference arm compensation plates were introduced. The thickness of the compensation plates was chosen so that the overall effective dispersion in both arms was almost equal. The dispersion of the external prism compressor was then adjusted so that the pulses at the output of the Michelson

*Corresponding author. (E-mail: feurer@qe.physik.uni-jena.de)

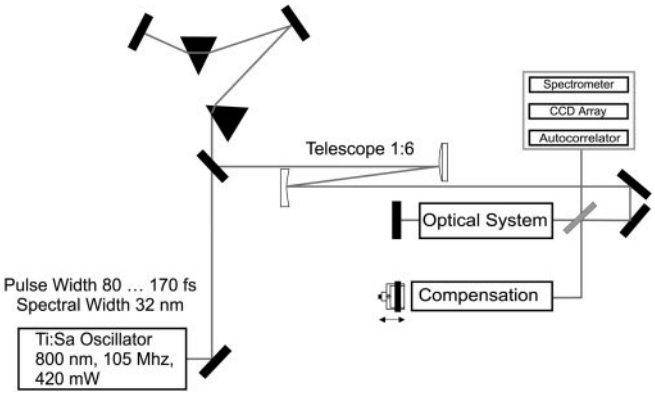

Fig. 1. The home-built Ti:sapphire oscillator delivers pulses at 800 nm, 105 MHz, and a spectral bandwidth of 36 nm. The pulses were sent in an external prism compressor and the beam diameter was subsequently magnified or demagnified before entering the Michelson interferometer using all reflective telescopes. Depending on the method the detection system at the output of the interferometer was either a CCD array, a spectrometer, or a scanning autocorrelator

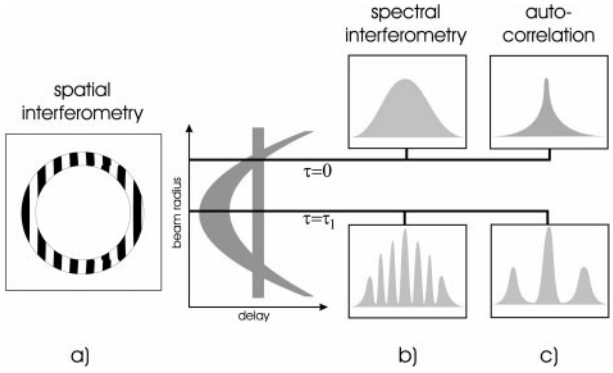

Fig. 2a–c. The basic concepts of the three methods are shown. For the first two methods the beam size was larger than the pupil size and in the case of the last technique the beam size was smaller than the pupil diameter. **a** Spatial interferometry: the plane pulse-front from the reference arm overlaps with the curved pulse-front from the object arm. Fringes due to a small tilt of the plane reference pulse are only visible when the two pulses overlap in time.**b** Spectral interferometry: the entrance slit of a spectrometer is scanned across the output of the Michelson interferometer. The delay between the two pulses can be inferred from the fringe separation. **c** Autocorrelation: the pair of pulses emerging from the output of the Michelson interferometer was measured by a commercial autocorrelator. The delay between the two pulses is extracted from the measured autocorrelation trace. The pair of objectives is then moved perpendicular to the optical axis in order to measure the delay as a function of the pupil radius

interferometer exhibited a minimum pulse duration. Depending on the technique at the output of the Michelson interferometer different detectors were used, namely a CCD array, a spectrometer, or a scanning autocorrelator. For the first two methods the beam was magnified so that the beam size was larger than the pupil of the objectives. In the case of the last technique the beam size had to be demagnified since the nonlinear detection system required a higher intensity.

(I) The first technique used was a conventional interferometric method similar to the one described in [10]. The optical element to investigate was placed in the object arm. The reference arm contained the compensation plates only, therefore, no pulse-front distortion occurs. By tilting the mirror of the reference arm a small angle was introduced between the two beams and interference fringes were visible at the output of the Michelson interferometer. The fringes were detected by a CCD array as a function of the beam radius r and the delay time τ between the two interferometer arms. Since the visibility of the fringes depends on the temporal overlap of the two pulses this technique may be used to measure the delay of the pulse-front as a function of the beam radius (see Fig. 2a). The position of the pulse maximum or pulse-front is defined as the location of the maximum visibility of the interference fringes. Therefore, the radial position of the pulse maximum for each delay time can be extracted from the measurements and the group delay may be inferred.

(II) For the spectral interferometry measurements the output of the Michelson interferometer was spatially scanned across the entrance slit of a spectrometer. Therefore, the spectral interference trace was measured as a function of the beam radius [7–9]. The recorded spectrum exhibits a modulation with a frequency that depends mainly on the temporal separation between the two pulses,

$$S(\omega, r) = A_1(\omega)^2 + A_2(\omega)^2 + 2\,A_1(\omega)A_2(\omega) \times \cos\left[\Phi_1(\omega) - \Phi_2(\omega) - \omega\tau(r)\right], \quad (1)$$

where $E_1(\omega) = A_1(\omega)\mathrm{e}^{\mathrm{i}\Phi_1(\omega)}$ and $E_2(\omega) = A_2(\omega)\mathrm{e}^{\mathrm{i}\Phi_1(\omega)+\mathrm{i}\omega\tau(r)}$ are the electric fields in the spectral domain of the laser pulses emerging from the two interferometer arms. The two pulses are separated by a time delay $\tau(r)$ which depends on the beam radius r (see Fig. 2b). The phase difference $\Phi_1(\omega) - \Phi_2(\omega)$ is assumed to be independent of the radius and close to zero due to the compensation of the dispersion. The length of one arm of the interferometer was varied for each radius r until the oscillations disappeared, i.e. both pulses overlapped in time ($\tau = 0$). Hence, from the distance the end mirror of the reference arm had to be moved, the group delay as a function of the beam radius can be inferred.

(III) The third method directly measures the effective group velocity of the microscope objectives as a function of the radius. The detection system was a commercial autocorrelator. Since this technique requires a higher intensity due to the nonlinear detection system the beam size was demagnified to about 1 mm diameter. Then a pair of identical microscope objectives (1:1 telescope) was mounted in the object arm of the interferometer. The pulse emerging from the object arm was delayed with respect to the pulse from the reference arm. Finally, an autocorrelation of the pair of pulses from the output of the interferometer was recorded. By analyzing the autocorrelation trace the temporal delay τ between the two pulses can be deduced. Due to the radius-dependent effective group delay, the delay between the two pulses depends on the position of the beam with respect to the pupil of the objective (see Fig. 2c). By moving the pair of objectives perpendicular to the optical axis the group delay as a function of the pupil radius can be measured. Due to the finite size of the laser beam the measured value is an average over the beam size.

2 Experimental results and discussion

Prior to the investigations of the microscope objectives a simple telescope consisting of two lenses was used. The focal lengths of the two BK7 lenses were $f_1 = 38$ mm and $f_2 = 54$ mm, respectively. The pair of lenses was mounted

in the object arm of the interferometer and a compensation plate in the reference arm. The prism compressor was adjusted so that the pulses emerging from the interferometer had a minimum temporal pulse duration. Figure 3a shows the fringe-averaged interferometric trace as a function of the delay time τ and the beam radius r for a double pass through the telescope. The fringe-averaged trace has been obtained by calculating the Fourier transform of the interferometric trace, filtering out the carrier frequency of the laser, and calculating the inverse Fourier transform. The intensity of the laser in all experiments was adjusted so that no spectral modulation due to self-phase modulation occurred. Clearly, the portions close to the optical axis are retarded with respect to the edges and the pulse-front delay exhibits a parabolic shape as expected from theory [10],

$$\tau(r) = -\frac{\lambda_0}{2c\, f_1 (n-1)} \left(1 + \frac{f_2}{f_1}\right) \frac{\mathrm{d}n}{\mathrm{d}\lambda}\, r^2 \quad \text{with} \quad r \in [0, r_0], \tag{2}$$

where c is the speed of light in vacuum and $\mathrm{d}n/\mathrm{d}\lambda$ is the dispersion of the lens material. The group delay $\tau(r)$ in (2) is calculated for a pulse traversing the telescope in a single pass. The telescope has been investigated using all three experimental methods. The delay of the pulse-front or the group delay is shown in Fig. 3b as a function of the beam radius. An excellent agreement between all methods and the theoretical prediction (2) is found. The slight deviation at the edges in the case of the autocorrelation technique is due to the fact that the beam size accepted by the autocorrelator was on the order of 1 mm. Clearly, in the case of the telescope chromatic aberration is the dominating effect. For all three techniques the accuracy of the measurements of ± 2 fs is limited by the translation stage that was used to scan the delay.

After carefully calibrating and testing all methods with the telescope consisting of two lenses, a number of widely used objectives in microscopy have been investigated. Most of them were placed in pairs in the object arm of the interferometer. In these cases, the beam passed one objective four times. Two objectives were used in an autocollimation arrangement (two passes). In the reference arm compensation plates were introduced in order to ensure almost equal effective dispersion in both interferometer arms. No special effort was undertaken to achieve the minimum time–bandwidth product. In Table 1 the time–bandwidth product is listed for all objectives investigated together with the number of passes and the extra elements, such as immersion oil or cover slides. Since some of the objectives are corrected in combination with a matching fluid and a cover slide, immersion oil or water and cover slides were used for these measurements. If matching fluid and cover slides were used these elements have also been considered in the ray-tracing calculations. The effect of the cover slide on the pulse-front distortion was investigated by Radewicz et al. [9].

The fringe-averaged interferometric trace of a Zeiss Plan Neofluar $20\times/0.5$ objective after four passes is shown in Fig. 4a. Although, the pulse-front distortion is reduced due to the chromatic correction of the system of lenses, a residual maximum group delay of (-12 ± 2) fs for a single pass is found. The maximum group delay corresponds to the difference of the group delay on the optical axis and the edge of the pupil. In Fig. 4b the group delay is shown as a function of the radius for all three techniques. Obviously, there is an excellent agreement between all methods applied. A second objective, namely a Zeiss LD Achroplan $40\times/0.6$ Korr. has been investigated, since for this objective ray-tracing calculations are available which allow for a comparison between theoretical calculations and experimental results. The results together with the calculations are displayed in Fig. 5. For this objective only the linear detection techniques have been used. An excellent agreement between the measured and the calculated values is found. Obviously, the group delay exhibits

Table 1. Time–bandwidth product (tbp) obtained at the output of both arms of the interferometer. The second column lists the number of passes through the objective and the third column finally lists the extra optical elements used. The cover slides were 140 μm thick

Optical system	tbp	passes	extra elements
Telescope	0.54	2	–
Plan Neofluar $20\times/0.5$	0.73	4	–
Plan Neofluar $40\times/1.3$ oil	0.88	4	2 cover slides plus immersion oil
Neofluar Epi-Plan $50\times/0.85$	0.62	2	–
C-Apochromat $40\times/1.2$ W Korr.	–	4	2 cover slides plus aqua dest.
LD Achroplan $40\times/0.6$ Korr.	0.59	2	–
Achroplan $40\times/0.75$ W	0.69	4	2 cover slides plus aqua dest.

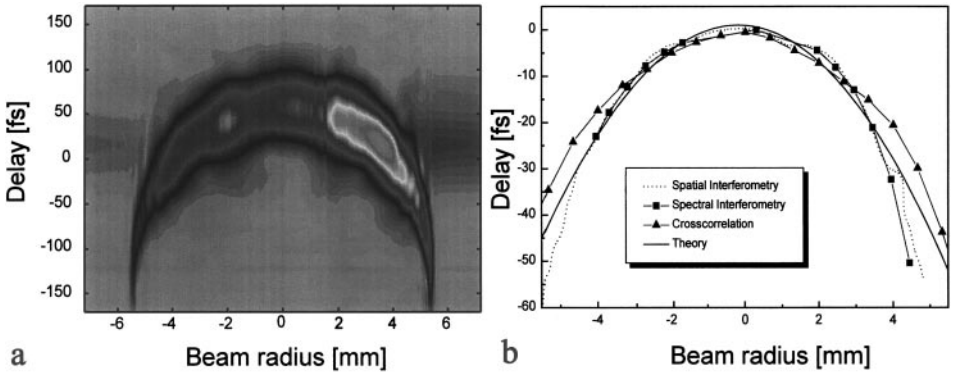

Fig. 3a,b. Pulse-front distortion of a telescope consisting of two BK7 lenses with a focal length of 38 mm and 54 mm, respectively. **a** The fringe-averaged interference trace after a double pass through the telescope is shown as a function of the beam radius r and the delay τ between the two interferometer arms. **b** From (**a**) the group delay for a single pass can be inferred and compared to the group delay obtained from the two alternative methods and the theoretical predictions

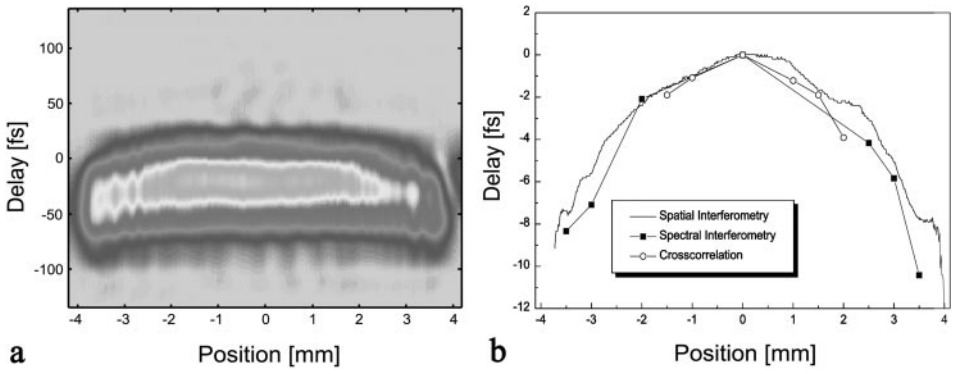

Fig. 4. **a** The fringe-averaged interference trace for a double pass through a Zeiss Plan Neofluar $20\times/0.5$ objective is shown as a function of the beam radius r and the time delay τ between the two interferometer arms. **b** Group delay as a function of the beam radius for a Zeiss Plan Neofluar $20\times/0.5$ objective. The results of the three experimental techniques are shown and an excellent agreement is found. The group delay exhibits a parabolic shape and the maximum group delay is (-12 ± 2) fs for a single pass

Table 2. The first two columns list the results for all measured optical systems using the two linear techniques. The values correspond to the group delay between the pulse on the optical axis and the edge of the pupil for a single pass in units of fs. The third column lists the derivative of the focal length with respect to the wavelength $\mathrm{d}f/\mathrm{d}\lambda$ at the center wavelength of 800 nm. In the next three columns the calculated group delay in fs is shown, first, using (3) and, second, a ray-tracing code without and with the tubus lens (TL)

	Experiment			Theory		
Optical system	Interf.	Spec.	$\frac{\mathrm{d}f}{\mathrm{d}\lambda}\Big\vert_{800\,\mathrm{nm}}$	(3)	no TL	TL
Plan Neofluar $20\times/0.5$	-11 ± 2	-13 ± 2	–	–	–	–
Plan Neofluar $40\times/1.3$ oil	13 ± 2	13 ± 2	-10.3	23.2	27.5	19.0
Neofluar Epi-Plan $50\times/0.85$	-15 ± 2	-12 ± 2	–	–	–	–
C-Apochromat $40\times/1.2$ W Korr.	23 ± 2	25 ± 2	-20.1	38.7	19.8	16.0
LD Achroplan $40\times/0.6$ Korr.	-23 ± 2	-24 ± 2	54.9	-26.4	-24.5	-26.5
Achroplan $40\times/0.75$ W	8 ± 2	–	-6.1	4.6	–	–

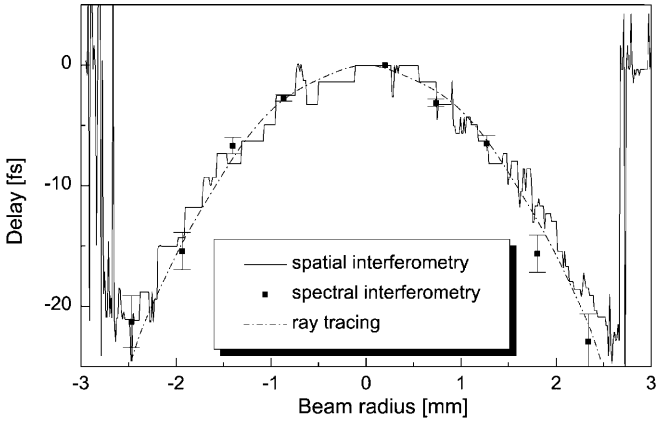

Fig. 5. Group delay as a function of the beam radius for a Zeiss LD Achroplan $40\times/0.6$ Korr. objective. The results from the interferometric and the spectral interferometry technique are compared to the theoretical results from optical ray-tracing calculations. The maximum group delay is (-23 ± 2) fs and an excellent agreement between theoretical and experimental results is found. Strong oscillations appear beyond the edge of the pupil $|r| > 2.47$ mm and mark the position of the pupil

an almost parabolic form with a maximum group delay of (-23 ± 2) fs.

The results for all objectives investigated are listed in Table 2. The first two columns list the maximum group delay for the two linear techniques, namely spatial and spectral interferometry. The maximum group delay corresponds to the difference of the group delay on the optical axis and the edge of the pupil. They were determined by extrapolating the measured group delay curves to the edge of the entrance pupil. The results of the autocorrelation measurements are not shown because with this method it was only possible to measure the group delay in the central part (see Fig. 4a) and extrapolating to the edge of the pupil would result in a large error.

For lens systems the maximum group delay due to chromatic errors can be estimated to

$$\tau_{\max} = -\frac{\lambda_0}{2c\,f_0^2}\,\frac{\mathrm{d}f}{\mathrm{d}\lambda}\,r_0^2, \tag{3}$$

where f_0 is the focal length at 800 nm. In the third column of Table 2 the first derivative of the focal length with respect to the wavelength at 800 nm is shown and in the fourth column the maximum group delay according to (3) is listed. Clearly, the sign of the maximum group delay changes as the sign of $\mathrm{d}f/\mathrm{d}\lambda$ changes which is in excellent agreement with the measurements. Since (3) only accounts for chromatic effects in some cases the absolute values differ quite substantially from the measured values. The Achroplan $40\times/0.75$ which was especially corrected for the IR wavelength region shows the smallest group delay.

Ray-tracing calculations account for almost all errors, such as chromatic and spherical aberration. Since all objectives are only fully corrected in combination with a tubus lens, the ray tracing calculations have been performed with and without the tubus lens. Obviously, the tubus lens adds a small constant amount of negative group delay to the maximum group delay on the order of a few fs. The measurements were all performed without the tubus lens. The calculated values are listed in the two last columns of Table 2. In all cases (except the Plan Neofluar $40\times/1.3$ oil) a good agreement between the measured and the calculated group delays is found. For the Plan Neofluar $40\times/1.3$ oil the measured value is about 100% smaller than the calculated value. Although no detailed studies have been performed this discrepancy might be caused by the immersion oil.

3 Conclusions

We have presented three experimental methods that are able to measure the pulse-front distortion introduced by lenses or

optical components consisting of lenses. In almost all cases good agreement is found comparing the results obtained by the three techniques with ray-tracing calculations. For high-numerical-aperture objectives the maximum group delay was between -20 fs and 20 fs. In agreement with the calculations the experiments show that the pulse-front distortion is mainly dominated by chromatic effects. A change of the sign of $\mathrm{d}f/\mathrm{d}\lambda$ causes a change of the sign of the group delay. In conclusion, for laser pulses shorter than 100 fs effects due to pulse-front distortion affect the temporal resolution. In order to overcome these limitations specially designed optical systems (objectives) must be used.

Acknowledgements. The authors are indebted to the Carl Zeiss Jena GmbH for providing the objectives and technical support and acknowledge fruitful and stimulating discussions with G. Szabo. The work has been funded by the Bundesministerium für Bildung und Forschung (FKZ: 13N7308/6). R. Netz gratefully acknowledges financial support from Carl-Zeiss-Schott-Förderstiftung.

References

1. W. Denk, J.H. Strickler, W.W. Webb: Science **248**, 73 (1990)
2. D.W. Piston, W.W. Webb: Biophysics **59**, 156 (1991)
3. S.W. Hell, M. Booth, S. Wilms, C.M. Schnetter, A.K. Kirsch, D.J. Arndt-Jovin, T.M. Jovin: Opt. Lett. **23**, 1238 (1998)
4. R. Wolleschensky, T. Feurer, R. Sauerbrey, U. Simon: Appl. Phys. B **67**, 87 (1998)
5. M. Mueller, J. Squier, R. Wolleschensky, U. Simon, G.J. Brakenhoff: J. Microsc. **191**, 141 (1998)
6. Z. Bor, Z.L. Horvath: Opt. Commun. **94**, 249 (1992)
7. J. Jasapara, W. Rudolph: Opt. Lett. **24**, 777 (1999)
8. L. Lepetit, G. Cheriaux, M. Joffre: J. Opt. Soc. Am. B **12**, 24 (1995)
9. C. Radewicz, M.J. la Grone, J.S. Krasinski: Opt. Commun. **126**, 185 (1996)
10. Z. Bor, Z. Gogolak, G. Szabo: Opt. Lett. **14**, 862 (1989)